The Rejection of QCD Jet Background to the Process $pp \longrightarrow \mathrm{H}^0 X(H^0 \longrightarrow \gamma\gamma)$ Using a Finely Segmented Crystal Calorimeter

pp ---> H0 X (H0 ---> gamma gamma)

K.Lübelsmeyer, D.Pandoulas, W.Wallraff, Y.Zeng
I. Physikalisches Institut, RWTH Aachen [1]
Germany

Aachen, Tech. Hochsch., I Phys. Inst.

E

Abstract

We present the results of a detailed simulation of QCD jet background to the process pp $\longrightarrow$ $\mathrm{H}^0\mathrm{X}(\mathrm{H}^0 \longrightarrow \gamma\gamma)$. Two cylindrical large radius crystal calorimeter designs with high granularity have been investigated. From an analysis of 2 million QCD events for each of the two detector options (inner radii of 2.5 m and 3 m) we obtain rejection factors of 7.5×10^7 and 6×10^8 respectively. The QCD jet background has thus been reduced to a level significantly lower than the irreducible background in both designs.

[1]Supported by the German Bundesminsterium für Forschung und Technologie under contract no. 056AC16P.

1.Introduction

The process $H^0 \longrightarrow \gamma\gamma$ provides the most promising signal to search for the Higgs boson in the mass region between 90 and 150 GeV [1] [2]. The final state consists of two isolated photons with high transverse momenta. At pp colliders there is a number of high rate processes leading to the same final state, the so called irreducible background: $gg \longrightarrow \gamma\gamma$, $q\bar{q} \longrightarrow \gamma\gamma$ and quark bremsstrahlung. Furthermore, because of fluctuations in jet fragmentation and in shower development in the calorimeter, the QCD jet processes can also lead to a similar experimental signature, particularly in case most of the energy of the parent parton is carried by a single π^0. The cross sections for these processes are listed in Table 1 [3] [4]. The irreducible background has a cross section which is three orders of magnitude higher than that of the signal. The signature for the Higgs particle is a peak in the two photon invariant mass spectrum over the continuous distribution of the background processes. The width of this peak is dominated by experimental factors. The detection of the signal sets severe requirements for the performance of the electromagnetic (e. m.) calorimeter [5].

Compared to the cross section of the irreducible background, the cross section of QCD jet processes is 1.6×10^6 times larger. This value, however, is subject to considerable theoretical uncertainties resulting from QCD higher order corrections [6] (200%) and uncertainties in the structure functions [7] (50%) and the fragmentation functions [8] (40%). The background to the Higgs signal resulting from QCD jet processes must at least be reduced to a level comparable to that of the irreducible background. Taking into account the uncertainties mentioned above, a suppression factor of the order of 10^7 is needed. For a reliable estimate of such a large rejection factor, a simulation based on a large data sample is required. In the following we present such an analysis performed for two CeF_3 crystal calorimeter geometries similar to those discussed by the L3P collaboration [2]. Preliminary results of this analysis using a simple shower shape cut have already been presented in Ref. [2].

2.The detector set up

Both crystal calorimeters considered here have a cylindrical geometry but

with different inner radii (R=2.5 m, 3 m). The pseudorapidity coverage is $|\eta| < 1.3$ and $|\eta| < 1$ respectively. The crystals point to the interaction region and have a front size of 3×3 cm^2 and a length of 41.25 cm (25 X_o for CeF_3). The resulting granularity is $\Delta\eta \times \Delta\phi = 0.012 \times 0.012$ at R=2.5m and 0.01×0.01 at R=3m. A tracking detector based on conventional technology in a solenoidal magnetic field of 3T (2T)[2] is assumed to fill the large inner cavity. The main parameters for both detector designs are shown in Table 2.

3.The analysis

Two million QCD jet events each have been generated using the PYTHIA program [9] with

$$P_T^{parton} > 40\ (40)\ \text{GeV},\ |\eta^{parton}| < 1.6\ (1.2) \qquad (1)$$

for the 2.5 m (3 m) design. Distribution (1) in Fig. 1(a,b) shows the cross section of QCD jet events as a function of the parton-parton invariant mass for the two detector geometries respectively.

For the following analysis a signal event is defined as a pp $\longrightarrow$ $H^0 + X$ with $H^0 \longrightarrow \gamma\gamma$ for $m_{H^0} = 100$ GeV overlayed with 19 minimum bias events[3], which are expected at standard LHC running conditions [11].

3.1 Preselection

To reject the majority of events which cannot possibly fake the $H^0 \longrightarrow \gamma\gamma$ decay, a preselection based on generator level information is first applied.

In the case of Higgs decay candidates, both photons are expected to have large transverse momenta: typically $P_T > 40$ GeV is demanded for the highest energetic and $P_T > 25$ GeV for the less energetic photon [1]. Clearly only jets with large e.m. energy can fake such photons. To impose a requirement on the e.m. energy content of the jet, we group the crystals into cells of size

[2]Numbers outside parentheses refer to the R=2.5m geometry, those in parentheses to the R=3m geometry.

[3]The parameters for the generation of the minimum bias events have been obtained by tuning the PYTHIA results to CDF and UA1/UA2 data [10]

0.12×0.12 in the $\eta - \phi$ plane and sum the energy of all photons (mostly from π^0 decays) and electrons in each cell. We then select events having:

$$\begin{aligned} &\geq 1 \text{ cell with e. m. energy } E_{em} > 30 \text{ GeV and} \\ &\geq 1 \text{ other cell with } E_{em} > 20 \text{ GeV} \end{aligned} \tag{2}$$

In total 12K (10K) events in the 2.5 m (3 m) options have been accepted in this step of the preselection, corresponding to distribution (2) in Fig.1(a,b) [4].

The e. m. energy in the jets comes mainly from π^o decays. In contrast to the well isolated photons from Higgs decay, most π^o's in jets are accompanied by several charged hadrons. The number of tracks in the central tracking device can be used to strongly reduce the remaining jet background.
To this purpose, we first combine into a single cluster all e. m. particles that are within a distance of 0.06 of each other in the $\eta - \phi$ plane. The cluster direction is determined by the center of gravity of its constituent particles and the nominal interaction point. For each cluster in a pair satisfying criterion (2), we then impose the requirement:

$$\mathrm{N}_{track} < 5 \tag{3}$$

where N_{track} is the number of charged tracks with $P_T > 2$ GeV in an area of 0.4×0.4 in the $\eta - \phi$ plane centered on the cluster direction.

Fig.2(a,b)[5] compares for QCD jet events and signal events the distribution of the number of charged tracks accompanying the two most energetic e. m. clusters. The distributions in Fig.2 suggest imposing the requirement $\mathrm{N}_{track} < 2$ in order to discriminate between Higgs decays and QCD jets. However, to take into account fragmentation uncertainties as well as central tracking inefficiencies, we have imposed the much looser condition (3). A total of 1004 (1270) events remain after this cut. Distribution (3) in Fig.1(a,b)

[4]We have checked that the steep fall-off of the fragmentation function leads to a negligible contribution of jet events with $25 < P_T^{parton} < 40$ GeV to our background event sample

[5]In this and all subsequent figures only the distributions for the 2.5m geometry are shown.

shows the cross section as a function of the invariant mass of the two most energetic e. m. clusters for the QCD events.

3.2 Calorimetric selection

We now investigate the differences in energy flow of QCD jets and signal photons observed with a crystal calorimeter. The events passing the preselection have been fully simulated in the crystal calorimeter geometries with the GEANT program package [12]. The two highest energetic e. m. shower candidates in the jets are reconstructed from the energy deposits with the same algorithm used for the reconstruction of Higgs decay photons [5]: The two crystals with the highest energy deposits are taken as the central crystals of the showers, provided the distance between them in the $\eta - \phi$ plane is greater than 0.2. The energy deposition $E_{5\times5}$ in the 5×5 crystal matrix around the central crystal is defined as the e. m. shower energy of photon candidates in the calorimeter.

The requirement on the transverse momentum of the two photons

$$P_T^{\gamma_1} > 40 \text{ GeV}, \; P_T^{\gamma_2} > 25 \text{ GeV} \tag{4}$$

used in the selection of $H^0 \longrightarrow \gamma\gamma$ events is also imposed on QCD jet events. 205 (211) events remain after this cut, leading to a suppression factor of 5 mainly in the low mass region ($m_{\gamma\gamma} < 100$ GeV). The cross section of these events corresponds to distribution (4) in Fig.1(a,b).

Compared to e. m. showers in jets, photons from Higgs decay are well isolated in the calorimeter. To suppress the background we therefore require that the peripheral shower energy fraction $((E_{0.4\times0.4} - E_{5\times5})/E_{5\times5})$ is limited:

$$\begin{aligned} &(E_{0.4\times0.4} - E_{5\times5})/E_{5\times5} < 0.08 \text{ for the higher energy jet} \\ &(E_{0.4\times0.4} - E_{5\times5})/E_{5\times5} < 0.12 \text{ for the lower energy jet} \end{aligned} \tag{5}$$

where $E_{0.4\times0.4}$ is the energy deposition in an area of 0.4×0.4 in the $\eta - \phi$ plane around the center of gravity of the e. m. shower. Fig.3(a,b) compares the distribution of the peripheral shower energy fraction for the two

QCD jets and the Higgs photons in signal events. For the higher energy jet 19 (15) events satisfy the isolation criterion. The corresponding number for the lower energy shower is 21 (14). The resulting suppression factor is 11 (14) for the higher energy jet and 10 (15) for the lower energy jet. The cross section corresponding to the remaining QCD jet background is shown as distribution (5) in Fig.1(a,b). It is derived from distribution (4) by scaling with the product of the suppression factors resulting from the application of the isolation criterion on each jet, since there is no correlation between the shower development in the individual jets.

At this point the QCD jet background has been reduced below the level of the irreducible one (Distribution (i) in Fig.1(a,b)). Exploiting the fine granularity and superior energy resolution of the calorimeter, further background suppression can be obtained by comparing the lateral shower development of jets to that of photons from Higgs decay. To this purpose, the impact point of the photon candidates on the central crystal is reconstructed with an improved center of gravity method [13]. The fraction of deposited energy in each crystal of the 5×5 matrix surrounding the central crystal depends on the position of the impact point. Dividing the surface of the central crystal in a 4×4 grid, leads to a classification of the photon candidates in 16 categories according to their impact point position. The distribution of the jet energy among the crystals of the 5×5 matrix is compared to that of Higgs photons in the same category. The comparison is made by means of a set of χ^2 functions [13] , defined as:

$$\chi_k^2 = \sum_{i=1}^{25} \frac{(x_{i,k} - x_{i,k}^{\gamma})^2}{(\sigma_x^{\gamma})_{i,k}^2}, \qquad k = 1...16$$

$$x_{i,k} = \frac{E_{i,k}}{E_{5\times5}}, \qquad x_{i,k}^{\gamma} = \frac{E_{i,k}^{\gamma}}{E_{5\times5}^{\gamma}}$$

Here $E_{i,k}$ ($E_{i,k}^{\gamma}$) is the energy deposited in the ith crystal of the matrix by a jet (photon) with impact point in the kth region of the central crystal and $(\sigma_x^{\gamma})_{i,k}$ is the r.m.s. value of the $x_{i,k}^{\gamma}$-distribution, determined in a separate high statistics study with GEANT [14]. The condition

$$\chi_k^2 < 60 \tag{6a}$$

leaves 8 (2) of the higher energy jets, while 2 (1) events pass the selection for the lower energy jet. The rejection of the lower energy jet is more significant, because on average the opening angles between the two photons from the decays of associated π^o's are larger. The finer granularity of the 3 m geometry results in more effective rejection of π^0's, since overlapping photon showers from the decay of single or several π^0's can be better distinguished from that of a single photon even at the energies characteristic for $H^o \longrightarrow \gamma\gamma$ decay.

A further suppression can be achieved by taking into account the energy deposition in the detectors behind the e. m. calorimeter, since for purely e.m. showers approximately only 3% of the photon energy leaks out of the back of a detector with a length of $25X_o$. For this energy, $E_{leakage}$, Fig.4(a,b) compares the fraction $E_{leakage}/E_{5\times5}$ for the two most energetic jets satisfying the isolation requirement (5) and for Higgs photons in signal events. Requiring for the fractional energy leakage

$$\begin{aligned} &E_{leakage}/E_{5\times5} < 0.08 \text{ for the higher energy shower} \\ &E_{leakage}/E_{5\times5} < 0.15 \text{ for the lower energy shower} \end{aligned} \tag{6b}$$

an additional suppression factor of 3 is obtained.

The final distribution (6) in Fig.1(a,b) is obtained by scaling distribution (5) by the product of the rejection factors resulting from the application of the shower shape and the energy leakage cuts (conditions (6a) and (6b)) on each of the two jets separately, leading to a residual QCD jet rate well below the level of the irreducible background. The error bars in distribution (6) reflect the uncertainties in the rejection factors due to statistical fluctuations and to the presently limited knowledge of the fragmentation process.

An overall suppression factor of 7.5×10^7 (6×10^8) is thus achieved for a calorimeter radius R=2.5 m (3 m).

The effect of the charged track veto (3) as well as the energy flow pattern requirements (5) and (6) on the signal efficiency is obviously approximately independent of the Higgs mass in the range $90 < m_H < 150$ GeV. Within

the geometrical acceptance of the detector, they lead to a signal selection efficiency of 93%. It should be noted that the transverse momentum requirements chosen here are optimized for $m_H = 100$ GeV . Taking those, as well as the detector coverage also into account, the overall efficiency for the Higgs signal is 27% (19%) at $m_H = 100$ GeV for the R=2.5 m (3 m) geometry.

Conclusion

The background suppression procedures described in this paper combine a fast rejection, based on simple track and energy deposit information (requirements 1-4) and implemented on the generator level, with a detailed analysis of the energy flow pattern of the events (requirements 5 and 6), accurately measured in a highly segmented crystal calorimeter. A total of 4 million QCD jet events have been analysed, half of them in a cylindrical calorimeter with an inner radius R=2.5 m, and the other half in a similar calorimeter with R=3 m. Suppression factors of 7.5×10^7 and 6×10^8 in total have been obtained for the two cases. Thus for both detector options the QCD jet background can be reduced to a level significantly lower than the irreducible background. It is evident that the larger radius detector design provides a better rejection power.

References

[1] C. Seez et al, ECFA-LHC Workshop, Aachen, CERN-TH 90-10 (1990) II-474.

[2] Letter of Intent of the L3P Collaboration, CERN/LHCC 92-5, LHCC/I3 (1992)

[3] Z. Kunszt and W. J. Stirling, ECFA-LHC Workshop, Aachen, CERN-TH 90-10 (1990) II-428.

[4] A. Djouadi, M. Spira and. P. M. Zerwas, Phys. Let. B 264 (1991) 440.

[5] M. Schöntag et al.,PITHA 93/26:"Higgs-detection in the decay channel $H^o \longrightarrow \gamma\gamma$ at the proposed experiment L3P at the future pp-collider LHC".

[6] R. K. Ellis, Proceedings of the XXVI International Conference on High Energy Physics, August 6-12,1992, Dallas, Texas. Edited by James R.Sanford, (p. 846).

[7] A. Mau, Diplomarbeit, RWTH Aachen: "Untersuchungen zum Signal-zu-Untergrund Verhältnis des $H^o \longrightarrow \gamma\gamma$ Zerfall".

[8] OPAL Collabration, M.Z. Akrawy et al., Phys. Lett. B247 (1990) 617.
OPAL Collabration, G. Alexander et al., Phys. Lett. B264 (1991) 467.
L3 Collabration, B. Adeva et al., Phys. Lett. B259 (1991) 199.

[9] T. Sjoestrand, PYTHIA manual version 5.6 (1990)

[10] G. Ciapetti, A. Di Ciaccio, ECFA-LHC Workshop, Aachen, CERN-TH 90-10 (1990) II-155.

[11] Design Study of the Large Hadron Collider, CERN 91-03.

[12] R. Brun et al, GEANT version 3.14.

[13] M. Micke, Doctoral Dissertation, RWTH Aachen, PITHA 90/03: "Pilotuntersuchungen zur Eichung des L3-BGO-Kalorimeters mit kosmischen Myonen".

[14] M. Schöntag, private communication.

Table 1: Comparison of cross sections($P_T^{max} > 40, P_T^{min} > 25$ GeV,$|\eta| < 1.3$)

Process	σ
$H^0 \longrightarrow \gamma\gamma$	2.8×10^{-11} mb
Irreducible background	0.95×10^{-8} mb
QCD 2 jets	1.5×10^{-2} mb

Table 2: The main parameters for the two detector options

Parameter	2.5 m Option	3 m Option
Radius	2.5 m	3 m
B-field	3 T	2 T
$\|\eta\|$ coverage	1.3	1.0
Granularity	0.012 x 0.012	0.01 x 0.01

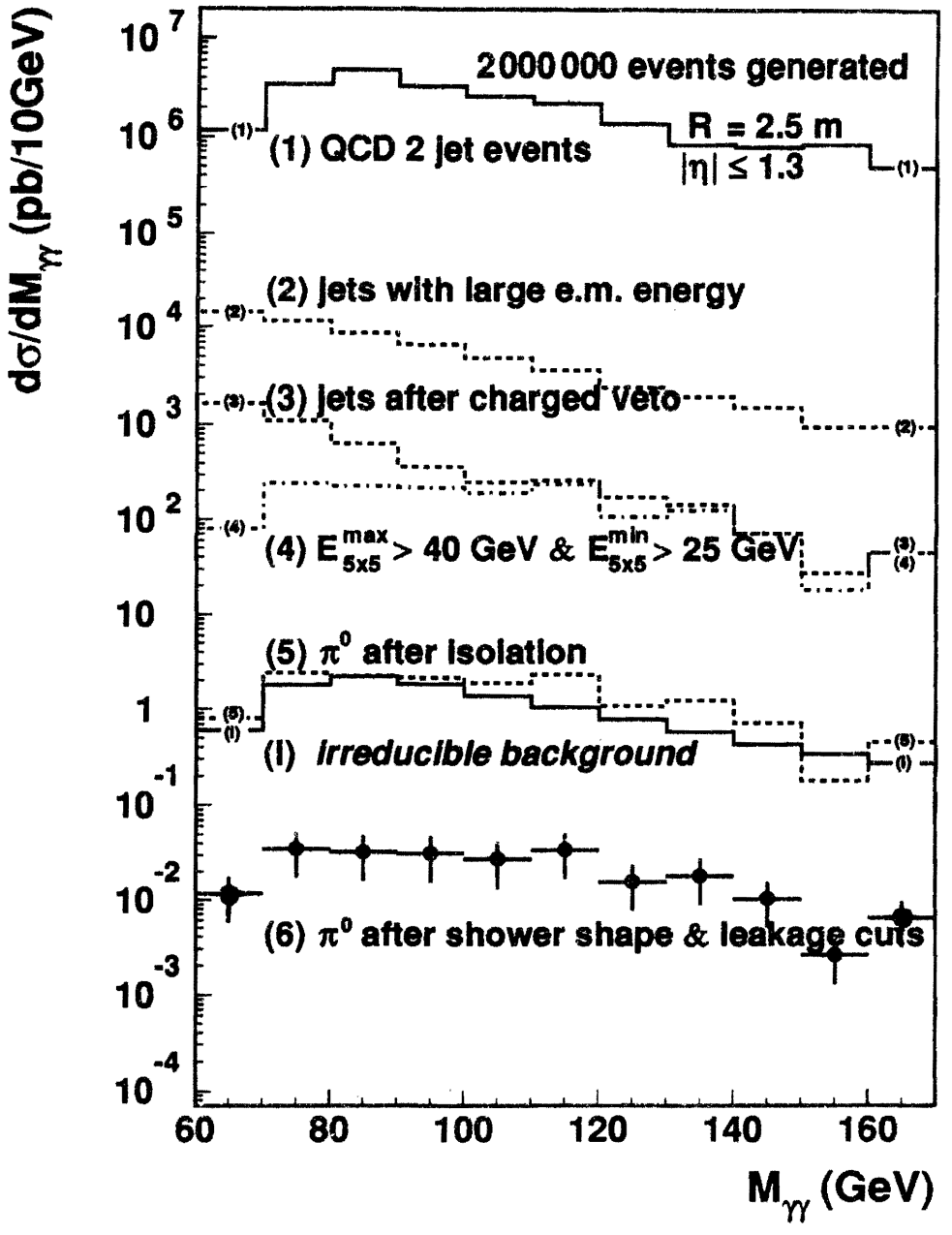

Figure 1a: The rejection of the QCD jet background in the 2.5 m geometry

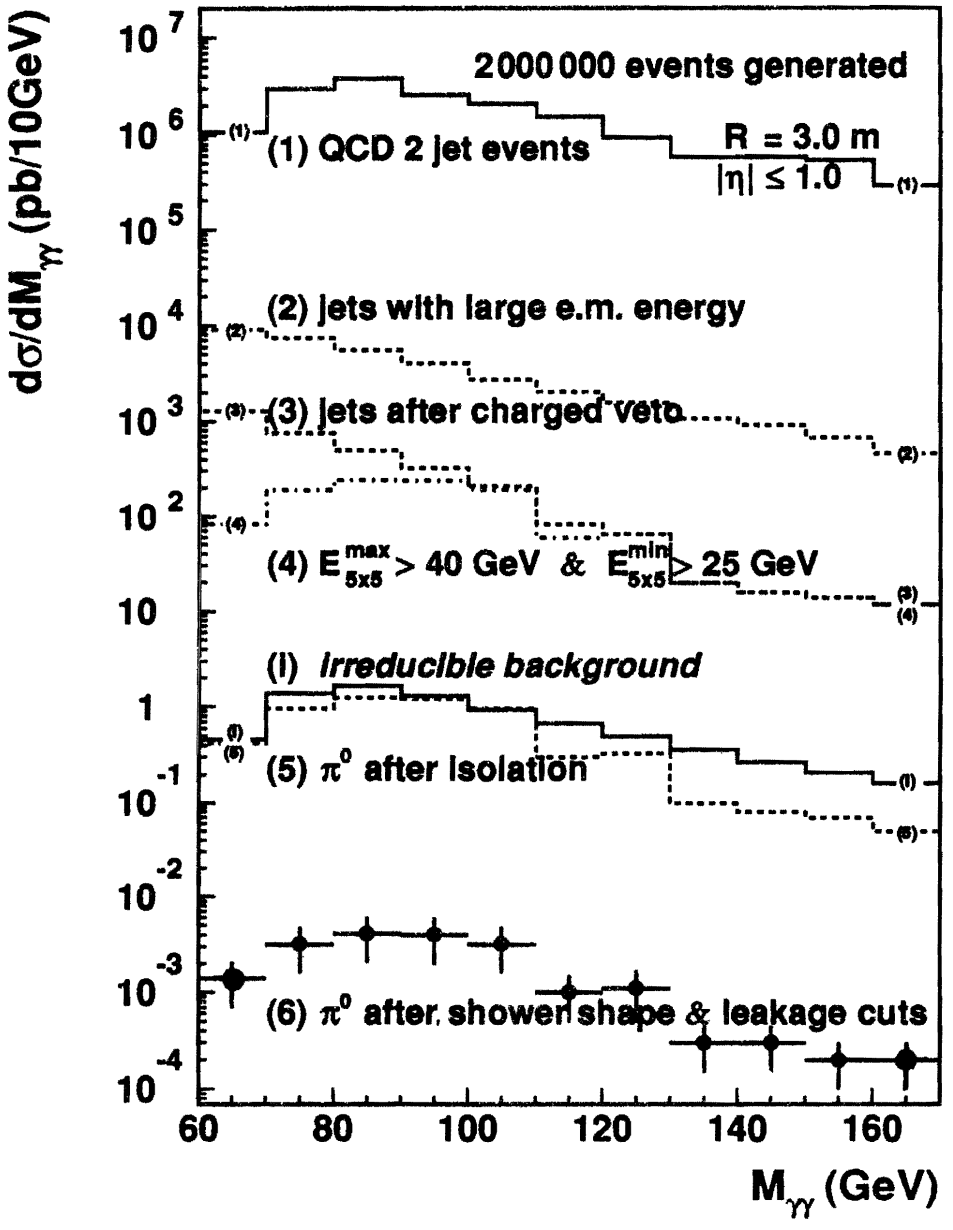

Figure 1b: The rejection of the QCD jet background in the 3 m geometry

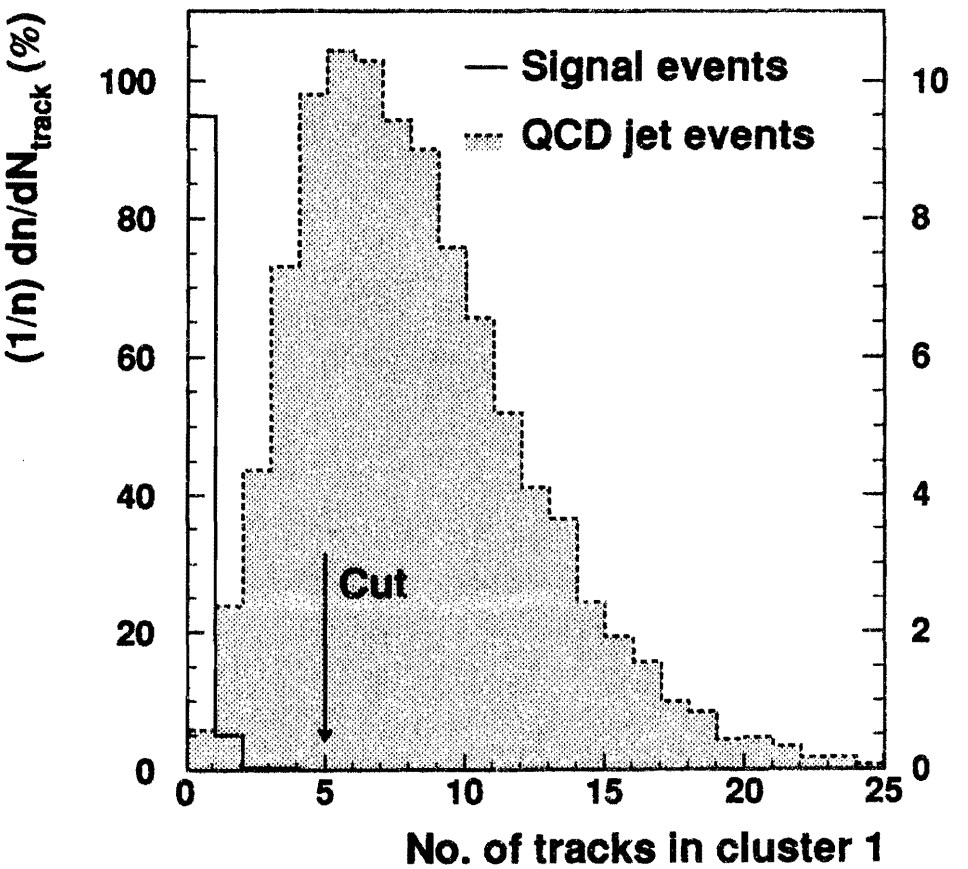

Figure 2a: Track number distribution ($P_T > 2$ GeV) for Higgs signal events (left scale) and QCD background (right scale). In this and all following figures the index '1' refers to the most energetic e.m. cluster/shower.

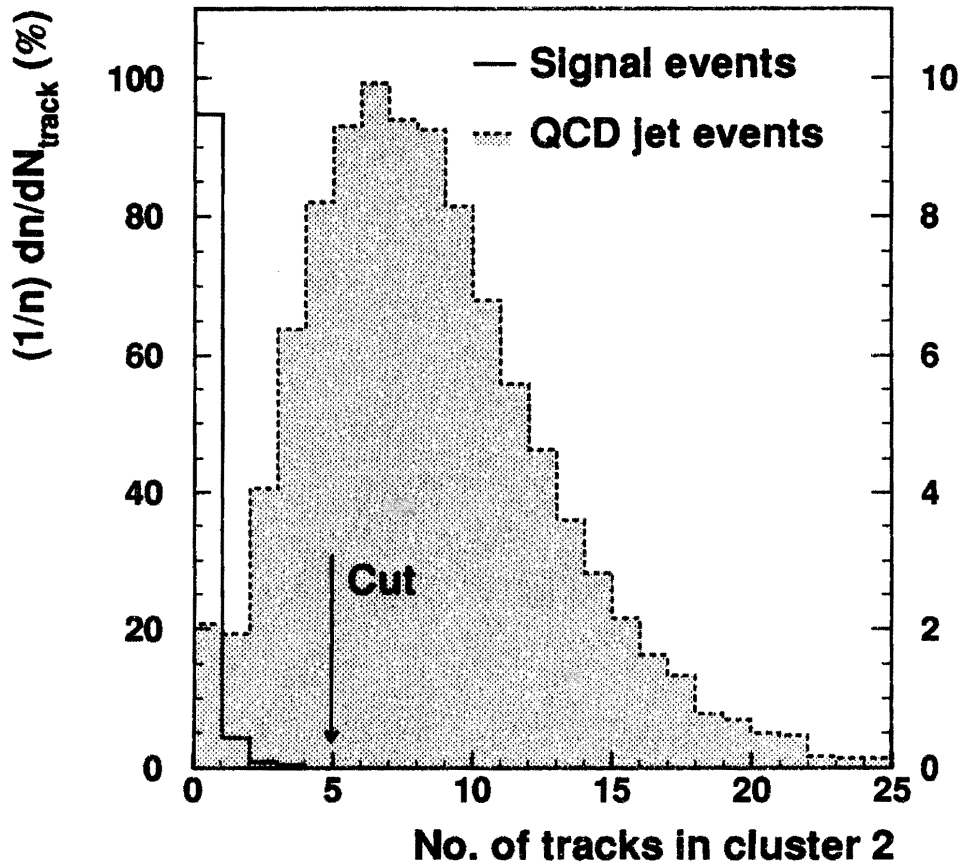

Figure 2b: Track number distribution ($P_T > 2$ GeV) for Higgs signal events (left scale) and QCD background (right scale). In this and all following figures the index '2' refers to the second highest energetic e.m. cluster/shower.

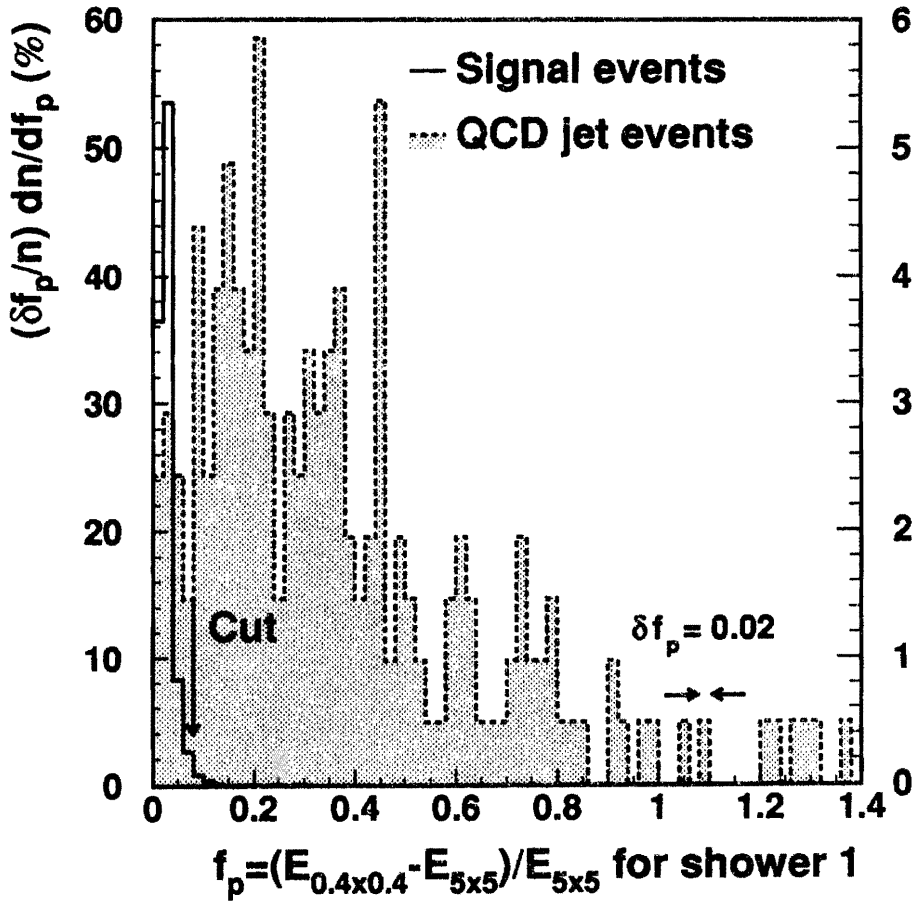

Figure 3a: The peripheral shower energy fraction for the higher energy shower in Higgs signal events (left scale) and QCD background events (right scale).

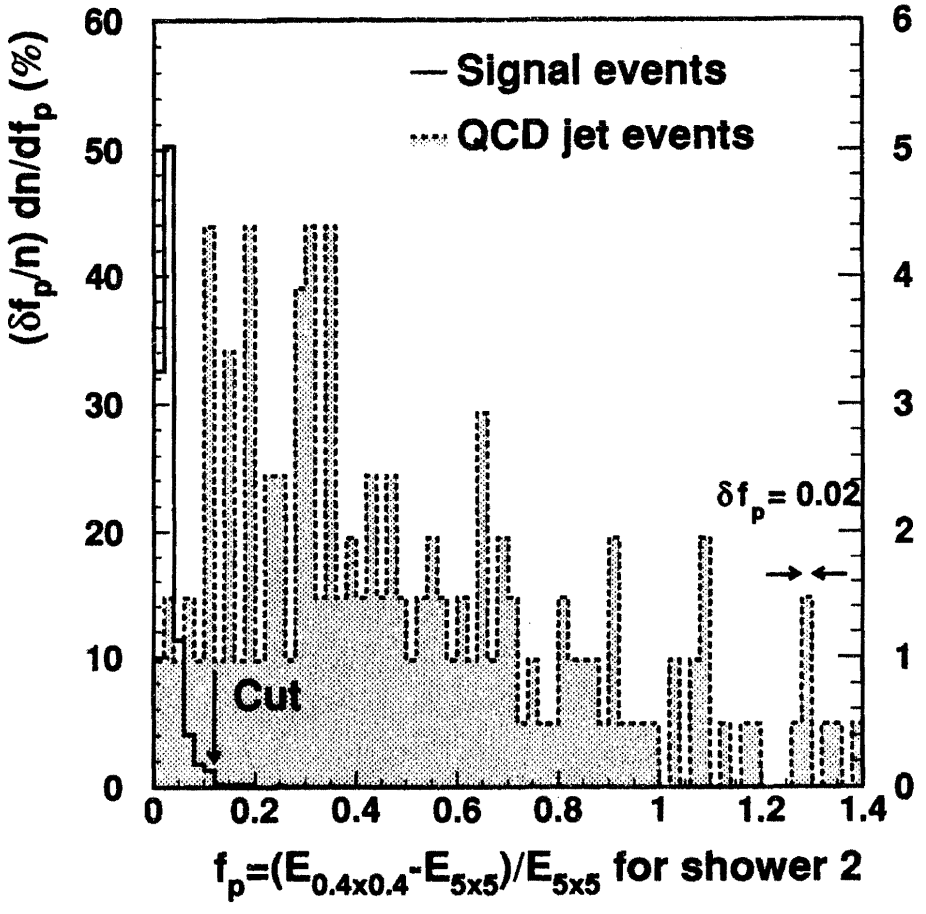

Figure 3b: The peripheral shower energy fraction for the lower energy shower in Higgs signal events (left scale) and QCD background events (right scale).

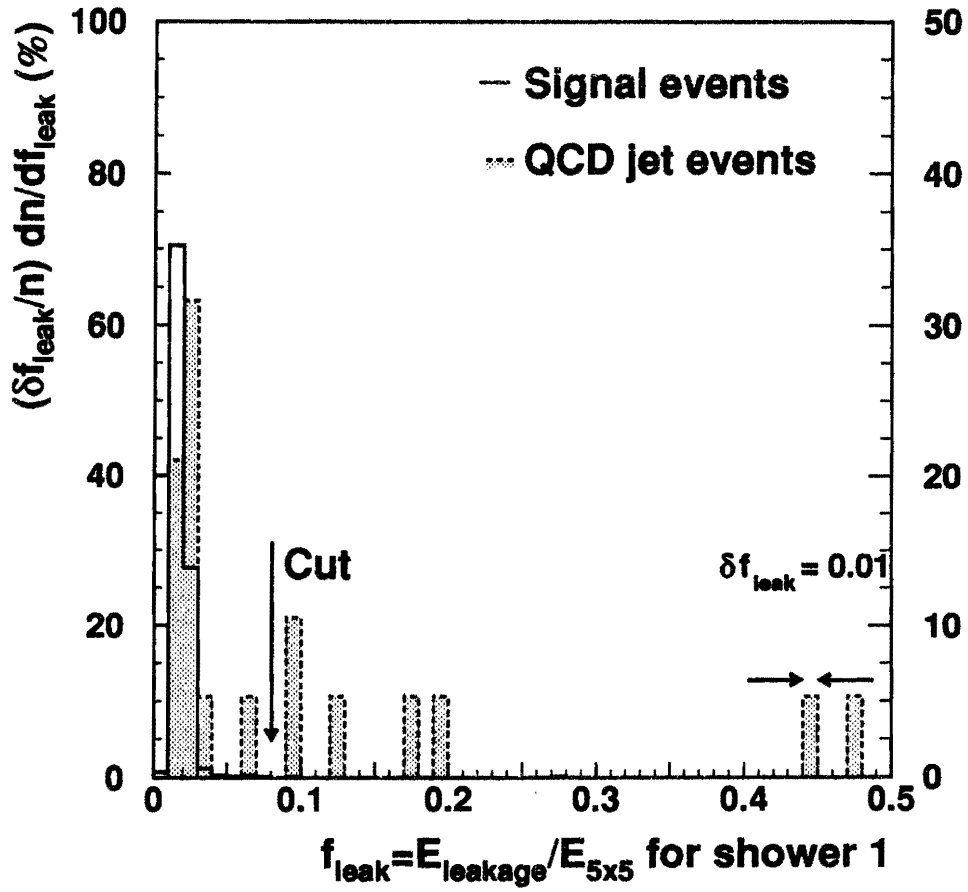

Figure 4a: The energy leakage fraction of the e.m. calorimeter; left scale: Higgs signal, right scale: QCD background.

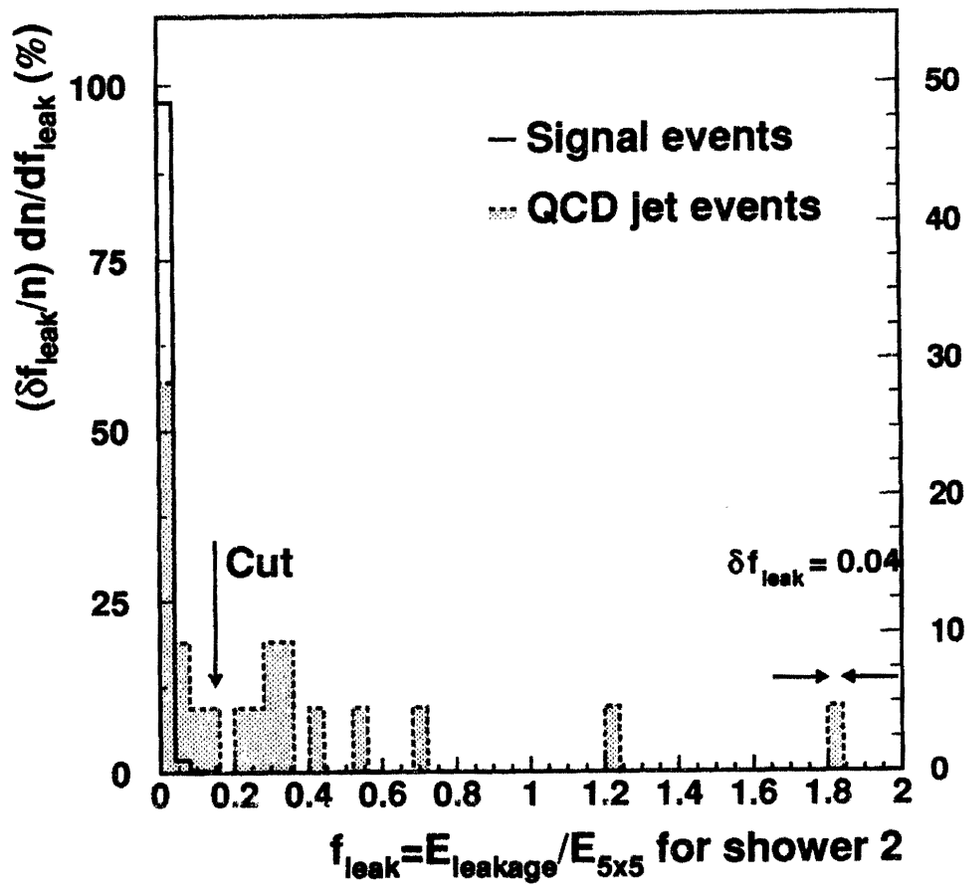

Figure 4b: The energy leakage fraction of the e.m. calorimeter; left scale: Higgs signal, right scale: QCD background.